Characteristic of femtosecond laser-pulsed digital holography*

Shi Bing-Chuan(石炳川)[a], Wang Xiao-Lei(王晓雷)[a]†, Guo Wen-Gang(郭文刚)[b], and Song Li-Pei(宋丽培)[a]

[a] Institute of Modern Optics, Key Laboratory of Optical Information Science and Technology, the Ministry of Education of China, Nankai University, Tianjin 300071, China

[b] Department of Basic Science, Institute of Military Traffic, Tianjin 300161, China

(Received 20 October 2014; revised manuscript received 3 January 2015; published online 20 June 2015)

Digital holography can be applied to ultrafast detection when a femtosecond laser pulse is used. In this paper, the interference process of two femtosecond laser pulses is studied and the recording process of the femtosecond laser pulsed digital hologram is simulated. Holograms at different recording angles are generated by integrating the instantaneous interference field. By analyzing the distribution of the reconstructed phase error, the characteristics of femtosecond laser pulsed digital holography are discussed.

Keywords: femtosecond digital holography, ultrafast information processing, phase reconstruction

PACS: 42.40.–i, 06.60.Jn, 42.30.Rx, 06.20.Dk **DOI:** 10.1088/1674-1056/24/8/084202

1. Introduction

In recent years, with the development of femtosecond laser pulse technology, femtosecond laser pulsed digital holography has been widely used. Compared with the conventional laser source, the femtosecond pulse has a very short duration, which means that it has a high time resolution in time-resolved pump-probe detection, short coherence length in multi-pulse interference, and strong peak power in laser ablation. In recent researches, the time-resolved femtosecond laser pulsed holography has been applied to detecting an ultrafast process,[1,2] such as laser interaction with materials, because it can provide much valuable experimental data due to its ability to record both amplitude and phase information. Digital holographic tomography[3–5] based on a short coherent pulse provides a new and effective way to avoid speckle noise. Instead of point-wise laser direct writing, femtosecond holographic lithography technology[6–9] has been used for machining the macro-grating structure and has potential applications in diffractive optical element lithography. Because of the short duration, the distribution of the interference field of femtosecond pulses is also different from that of a continuous laser, while the distribution is critical to digital holographic recording. Although some researches have been done on femtosecond digital holography,[10–12] the characterization and processing method show less difference. In this paper, we characterize the temporal integrating process of femtosecond laser pulsed interference and simulate its ability to make holographic recording in a specific case.

2. Analysis

Formed by multi-longitudinal mode locking, lots of frequency components are included in a pulse. Generally we assume that the amplitudes of the longitude modes have a symmetric Gaussian distribution, so the pulse envelope, which is obtained by the Fourier transform of the longitude modes, is Gaussian shaped in the time domain. In this case, the phase term can be expressed as a monochromatic wave of the central frequency. So the laser pulse can be expressed as

$$E(z,t) = \exp\left[-\frac{2\ln 2}{\Delta t^2}\left(t-\frac{z}{c}\right)\right] \times \exp\left[-\mathrm{j}\left(\omega_0 t+\varphi_0-\frac{\omega_0 z}{c}\right)\right], \quad (1)$$

where Δt is the pulse duration, ω_0 is the central frequency, φ_0 is the initial phase, and the pulse propagates in the Z direction.

Generally, the quadratic phase in the X–Y plane will be greatly weakened in the beam expanding process, thus no longer be considered. Assuming that the beam radius of the Gaussian beam is R, the amplitude distribution in the X–Y plane is

$$E(x,y) = E_0 \exp\left[-\frac{x^2+y^2}{R^2}\right]. \quad (2)$$

Based on Eqs. (1) and (2), the spatial and temporal expression of the Gaussian pulse amplitude is

$$E(x,y,z,t) \propto E_0 \exp\left[-\frac{x^2+y^2}{R^2}\right] \exp\left[-\frac{2\ln 2}{\Delta t^2}\left(t-\frac{z}{c}\right)^2\right] \times \exp\left[-\mathrm{j}\left(\omega_0 t+\varphi_0-\frac{\omega_0 z}{c}\right)\right]. \quad (3)$$

Figure 1 shows the schematic diagram of the interference process by two femtosecond pulses. In Fig. 1, pulses E_1 and

*Project supported by the National Natural Science Foundation of China (Grant No. 61275133).

†Corresponding author. E-mail: wangxiaolei@nankai.edu.cn

© 2015 Chinese Physical Society and IOP Publishing Ltd

E_2 are distributed in coordinate systems (X, Y, Z) and (X', Y', Z') respectively:

$$E_1(x,y,z,t) \propto E_0 \exp\left[-\frac{x^2+y^2}{R^2}\right] \exp\left[-\frac{2\ln 2}{\Delta t^2}\left(t-\frac{z}{c}\right)^2\right] \times \exp\left[-\mathrm{j}\left(\omega_0 t+\varphi_0-\frac{\omega_0 z}{c}\right)\right], \quad (4)$$

$$E_2(x',y',z',t) \propto E_0 \exp\left[-\frac{x'^2+y'^2}{R^2}\right] \exp\left[-\frac{2\ln 2}{\Delta t^2}\left(t-\frac{z'}{c}\right)^2\right] \times \exp\left[-\mathrm{j}\left(\omega_0 t+\varphi_0-\frac{\omega_0 z'}{c}\right)\right], \quad (5)$$

where coordinate system (X', Y', Z') is rotated by a small angle α around the X axis with respect to coordinate system (X, Y, Z), thus the beam angle is α. The relationship between the two coordinates is

$$\begin{aligned} x' &= x, \\ y' &= y\cos\alpha + z\sin\alpha, \\ z' &= z\cos\alpha - y\sin\alpha. \end{aligned} \quad (6)$$

As the pulses propagates, the amplitude of the femtosecond pulse changes rapidly, so the interference process lasts a very short time, and the instantaneous intensity is

$$I_{\mathrm{ins}}(x,y,z_0,t) = |E_1(x,y,z_0,t)+E_2(x,y,z_0,t)|^2. \quad (7)$$

The interferogram recorded by the charge coupled device (CCD) is:

$$I_{\mathrm{int}}(x,y) = \int_T |E_1(x,y,z_0,t)+E_2(x,y,z_0,t)|^2 \,\mathrm{d}t. \quad (8)$$

For a certain pixel of the charge coupled device (CCD), the phase difference between pulses E_1 and E_2 is constant, so the difference in pixel energy is just caused by the difference in pulses' amplitude. Given in the following is a detailed illustration of this process.

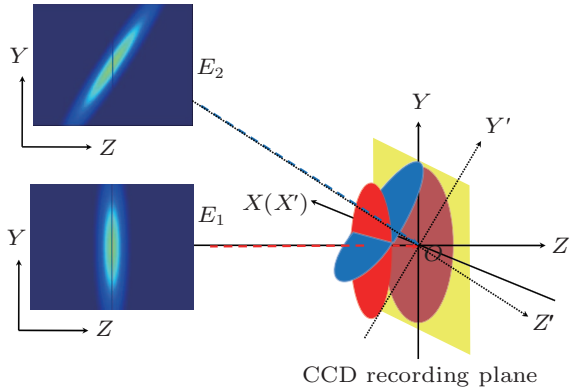


Fig. 1. (color online) Interference and recording of femtosecond laser pulses.

Figure 2 shows the overlapping process of two femtosecond laser pulses in the $x = 0$ plane. The photosensitive surface of the CCD is placed in the plane at $z = 0$. The pulse duration is set to be 50 fs, the wavelength is 800 nm and the pulse amplitude is 0.5, the radius of the incident beam is 3 mm, the angle between two beams α is 0.01 rad and the time when the amplitude peak of a single pulse arrives at the $z = 0$ plane (the vertical center line in Fig. 2) is set to be 0 fs. Corresponding to Fig. 2, the normalized intensity of the interference signal is shown in Fig. 3. In Figs. 2 and 3, different scales of Z and Y axes are adopted to obtain a better demonstration effect, where the Y axis ranges from -5 mm to 5 mm and the Z axis ranges from -100 μm to 100 μm.

As can be seen in Fig. 2, the pulse amplitudes in the recording plane are not always equal, so the instantaneous interference signal is rapidly changing in the plane. Figure 3 shows the changing process of the relative position between the signal and the recording plane.

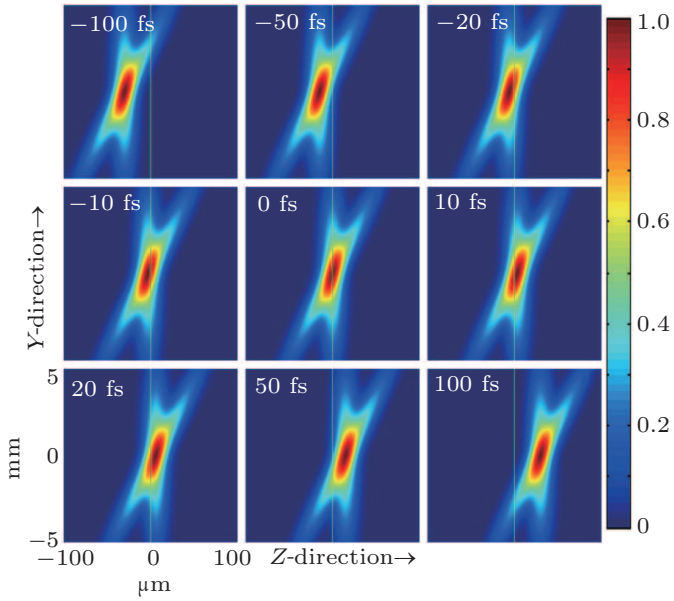


Fig. 2. (color online) Amplitude overlapping of two pulses at different times.

In Fig. 2, we can see that from -100 fs to -50 fs, part of the oblique incident pulse E_2 arrives at the recording plane while the normal incident pulse E_1 is far from it. So there is no interference fringe as shown in Fig. 3. At about -50 fs, the front of pulse E_1 arrives and is superimposed on E_2, thus interference fringes are generated in Fig. 3. From -50 fs to 0 fs, the interference signal increases as the pulse amplitude increases. At 0 fs the interference signal reaches its maximum. From 0 fs to 50 fs, the interference signal decreases as the amplitudes of pulse E_1 and pulse E_2 decrease. At about 50 fs, the tail of pulse E_1 escapes from the recording plane while part of pulse E_2 does not yet. So after 50 fs, the interference signal in the recording plane disappears and the rest of the energy of E_2 is only contributed to background intensity.

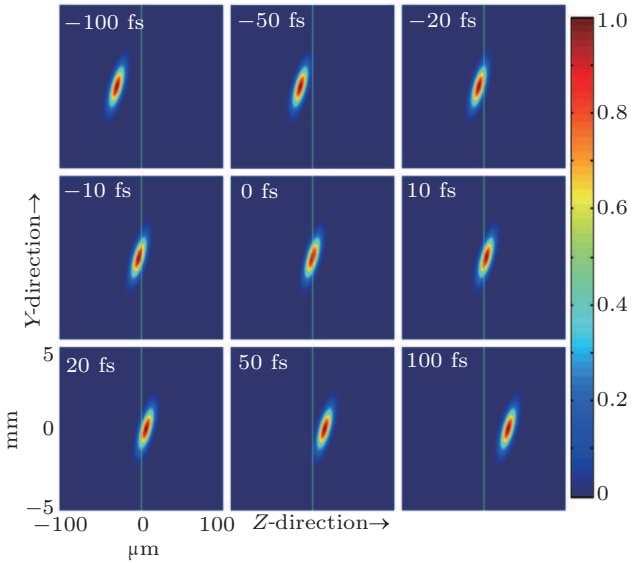


Fig. 3. (color online) Intensity distributions of interference signal at different times.

3. Simulation and discussion

To realize the characteristic performance of femtosecond laser pulsed digital holography, image digital holographic recording and reconstruction process are simulated.[13]

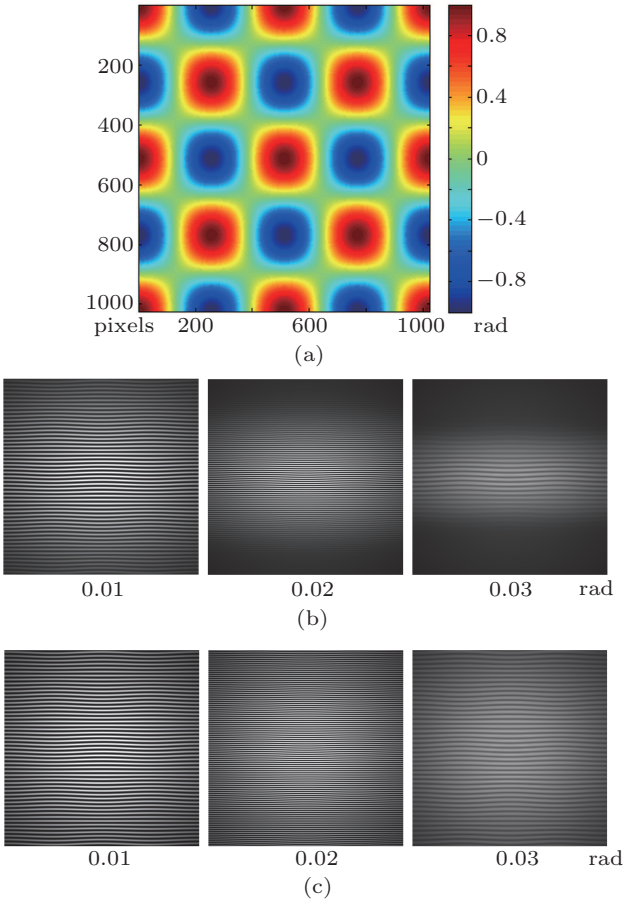


Fig. 4. (color online) (a) Two-dimensional phase object, (b) holograms recorded by femtosecond pulses, and (c) holograms recorded by continuous laser.

A two-dimensional cosine phase object is chosen as an object to be recorded as shown in Fig. 4(a). The holograms are recorded by a virtual CCD (1024 pixels×1024 pixels, 4 μm×4 μm, 8 bit) at different angles between two beams. For example, only holograms with the values of angle α being 0.01 rad, 0.02 rad, and 0.03 rad are given in Fig. 4(b). For comparison, holograms generated by continuous laser are also given in Fig. 4(c).

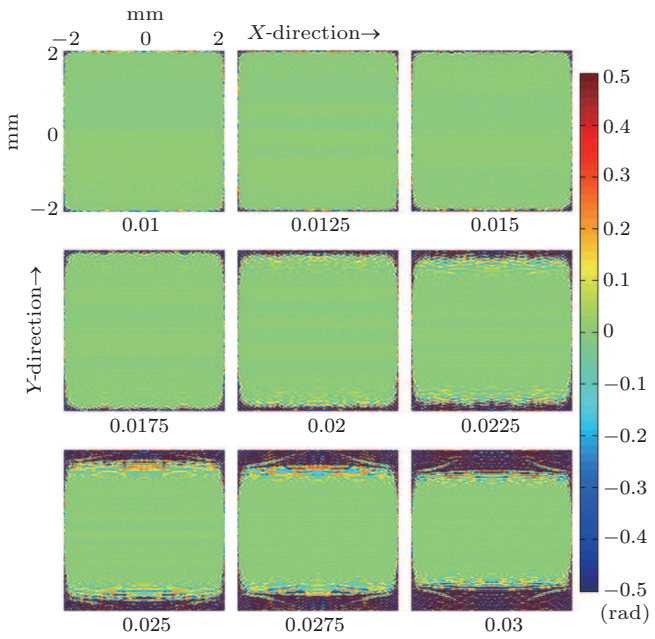


Fig. 5. (color online) Error distributions of reconstructed phases of femtosecond pulsed holograms.

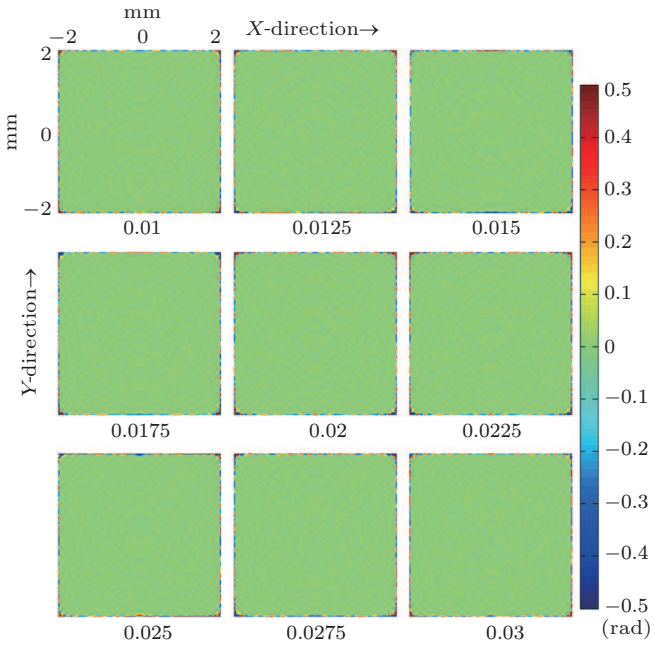


Fig. 6. (color online) Error distributions of reconstructed phases of continuous laser holograms.

Compared with the holograms generated by the continuous laser in Fig. 4(c), the fringe of femtosecond pulsed holograms in Fig. 4(b) has a lower edge contrast with the increase

of angle α. We reconstruct the femtosecond pulsed holograms and the continuous laser holograms, and the error distributions of the reconstructed phase are shown in Figs. 5 and 6 respectively. A Hanning window[14] is used in Fourier transform in order to reduce frequency spectrum leakage.

In order to display the error value we are concerned with, in Figs. 5 and 6 the maximum and minimum value are limited to 0.5 rad and -0.5 rad respectively, thus phase errors greater than 0.5 rad or less than -0.5 rad are just shown to be 0.5 rad or -0.5 rad respectively.

As shown in Fig. 5, when the angle α between two beams is less than 0.015 rad, the points of phase error are limited on the edge of the reconstructed phase map. As α increases to 0.0175 rad, the points of phase error expand and have a tendency that they are connected into a region in the Y axis direction. As α increases to 0.02 rad, a significantly different region consisting of many error points appears on each of both sides in the Y direction. The error distributions in Fig. 5 indicate that the phase error region expands obviously as the angle α between two beams increases. However, from Fig. 6 it can be seen that the phase error derived from holograms generated by continuous laser is not influenced by increasing angle α between two beams.

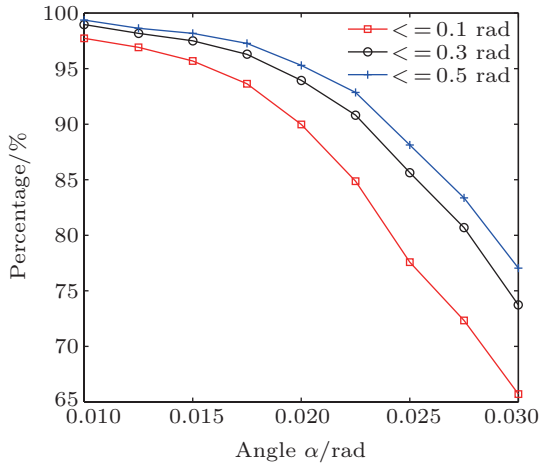


Fig. 7. (color online) Statistics of phase error points.

Figure 7 shows the statistics of Fig. 5, in which the percentages of phase error points less than 0.5 rad, 0.3 rad, and 0.1 rad are plotted with respect to the angle between two beams respectively. When the angle is not more than 0.015 rad, up to 95% points can be reconstructed in high accuracy (phase error<=0.1 rad). Obviously there exists a slope change between 0.015 rad and 0.025 rad. When the angle is greater than 0.025 rad, the percentage decreases linearly. These three sections of the phase error points are corresponding to the expanding process mentioned above. So the angle is less than 0.015 rad, and we can infer that the phase error points are just caused by the Gibbs effect at the edge, namely, the reconstructed phase derived from femtosecond laser pulsed digital hologram has a high accuracy. As the angle is greater than 0.025 rad, the percentage decreases sharply in Fig. 7, which is caused by non-interference of the two pulses.

4. Conclusions

According to the above simulations and analyses, we can know that the recording area becomes smaller with the increase of the angle between two beams, so the interference recording area of femtosecond laser pulsed digital holography is limited. The limitation comes from the limited spatial and temporal distribution of femtosecond laser pulses. Although neither noise nor fluctuation is not considered, the simulation and analysis results above can be a guide to the implementation of the femtosecond laser pulsed digital holography.

References

[1] Hu H, Wang X and Zhai H 2011 *Opt. Lett.* **36** 124
[2] Hayasaki Y, Isaka M, Takita A and Juodkazis S 2011 *Opt. Express* **19** 5725
[3] Cuche E, Poscio P and Depeursinge C 1997 *J. Opt.* **28** 260
[4] Martínez-León L, Pedrini G and Osten W 2005 *Appl. Opt.* **44** 3977
[5] Yuan C, Zhai H, Wang X and Wu L 2007 *Opt. Commun.* **270** 176
[6] Jia T, Baba M, Suzuki M, Ganeev R A, Kuroda H, Qiu J and Xu Z 2008 *Opt. Express* **16** 1874
[7] Li Y, Yamada K, Ishizuka T, Watanabe W, Itoh K and Zhou Z 2002 *Opt. Express* **10** 1173
[8] Misawa H, Kondo T, Juodkazis S, Mizeikis V and Matsuo S 2006 *Opt. Express* **14** 7943
[9] Li Y, Watanabe W, Yamada K, Shinagawa T, Itoh K, Nishii J and Jiang Y 2002 *Appl. Phys. Lett.* **80** 1508
[10] Maznev A A, Crimmins T F and Nelson K A 1998 *Opt. Lett.* **23** 1378
[11] Ansari Z, Gu Y, Tziraki M, Jones R, French P M W, Nolte D D and Melloch M R 2001 *Opt. Lett.* **26** 334
[12] Ma Z, Yang Y, Zhai H and Chavel P 2013 *Opt. Lett.* **38** 49
[13] Brandt G B 1969 *Appl. Opt.* **8** 1421
[14] Harris F J 1978 *Proc. IEEE* **66** 51